Supplemental Data

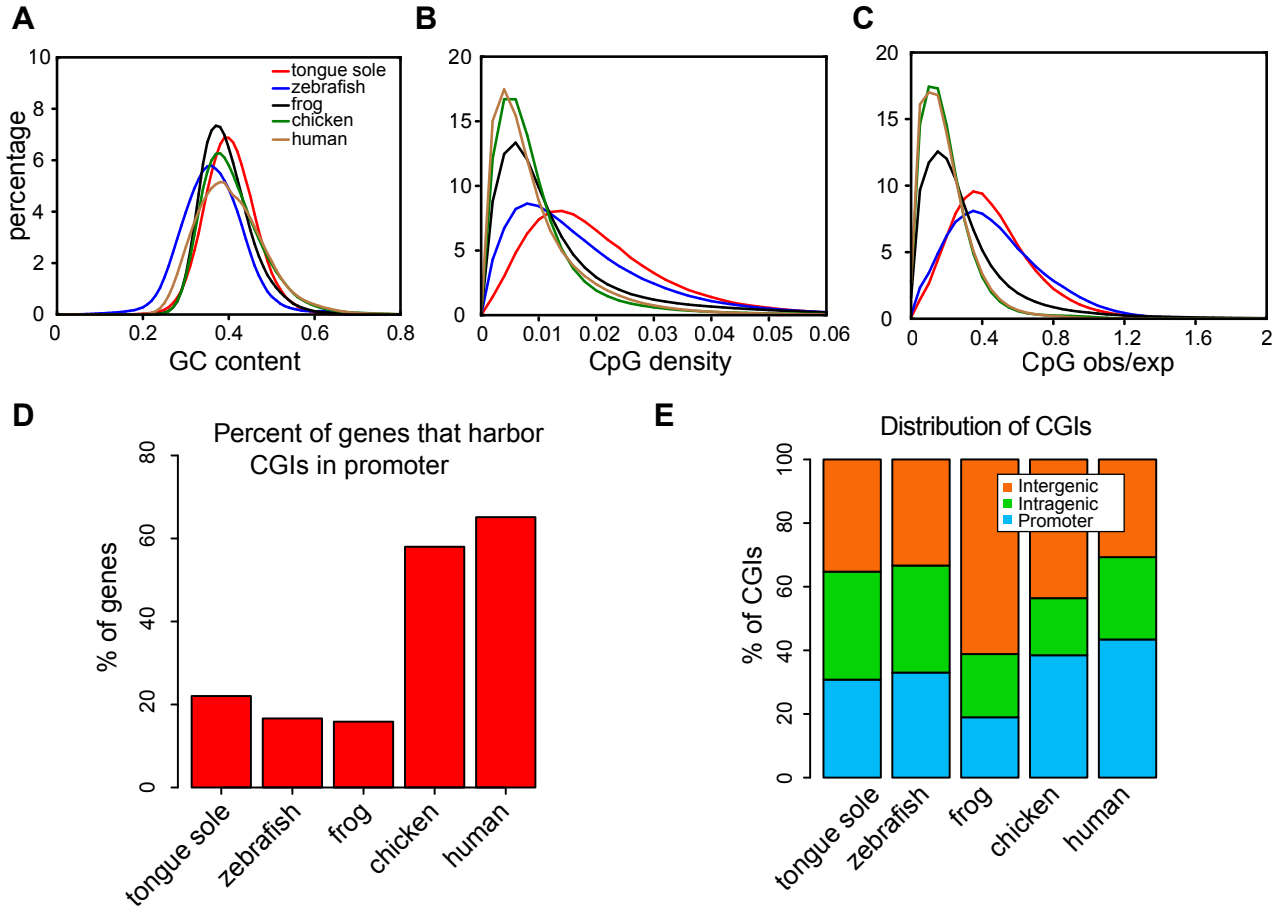

Figure S1. Comparison of genomic characteristics between tongue sole and other vertebrates. (**A**) GC content, (B) CpG density and (C) CpG o/e of the genomes of tongue sole (*C. semilaevis*), zebrafish (*D. rerio*), frog (*X. tropicalis*), chicken (*G. gallus*) and human (*H. sapiens*) calculated by 500-bp non-overlap sliding windows. For a given window, where *nC*, *nG* and *nCpG* refer to the number of observed C, G and CpG and *l* refers to the length of the window, GC content is calculated as (*nC* + *nG*) / *l*, CpG density is calculated as *nCpG* / (*l* - 1), and CpG o/e is calculated as *nCpG* / (*nC* * *nG*) * (*l* * *l*) / (*l* - 1). (**D**) Percentage of genes that harbor one or more CGIs in promoter regions. CGIs of tongue sole were identified by makeCGI (version 1.2, http://rafalab.jhsph.edu/CGI/) (Wu et al. 2010), and CGIs of zebrafish, frog, chicken and human were downloaded from UCSC Table Browser (http://genome.ucsc.edu/). (**E**) Genomic distribution of CGIs in different species. In general, the characteristics of the tongue sole genome are similar to that of zebrafish, e.g. both the genomes of tongue sole and zebrafish have higher CpG density and CpG o/e than that of frog, chicken and human, and have much fewer genes that contain CGIs in promoter regions compared with chicken and human.

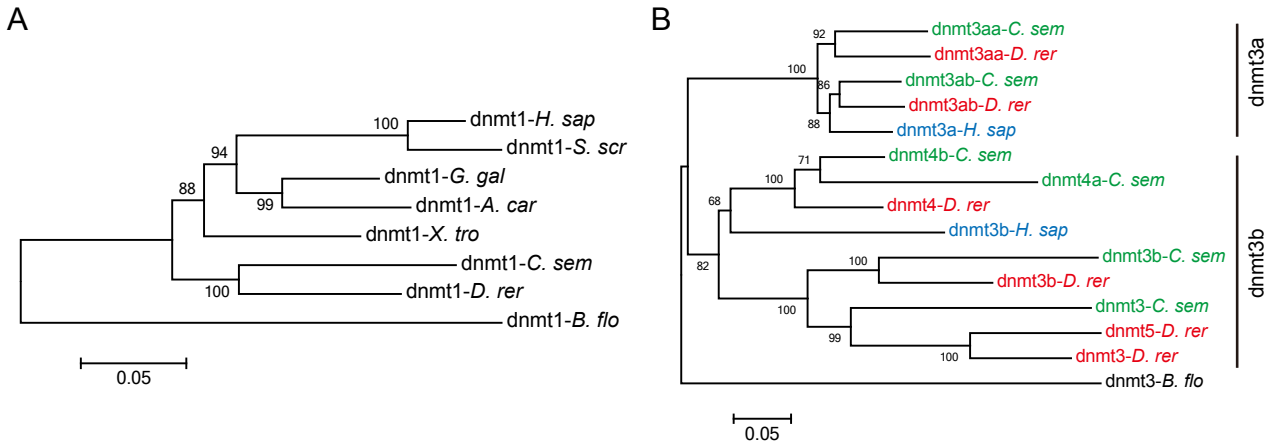

C

C. sem gene	*C. sem* length (aa)	tongue sole vs zebrafish				tongue sole vs human			
		D. rer gene	Align bg	Align ed	Identity	*H. sap* gene	Align bg	Align ed	Identity
dnmt1	1,493	dnmt1	1	1,493	78.02	dnmt1	220	1,488	73.12
dnmt3	1,226	dnmt3	637	1,226	57.38	dnmt3b	638	1,226	52.39
dnmt3b	823	dnmt3b	110	823	56.98	dnmt3b	216	853	67.55
dnmt4a	517	dnmt4	1	517	70.19	dnmt3b	4	517	59.74
dnmt4b	1,434	dnmt4	782	1,434	54.66	dnmt3b	839	1,434	54.56
dnmt3aa	820	dnmt3aa	129	819	77.76	dnmt3a	96	819	79.08
dnmt3ab	1,015	dnmt3ab	2	1,015	72.94	dnmt3a	332	1,015	85.26

Figure S2. *Dnmt* genes of tongue sole. (**A**) Phylogenetic tree of the dnmt1 protein sequences in different vertebrates. Dnmt1 of *B. floridae* was selected as the outgroup. As observed in other vertebrates, the tongue sole genome encode only one *dnmt1* gene. (**B**) Phylogenetic tree of the dnmt3 families in different vertebrates. Dnmt3 of *B. floridae* was selected as the outgroup. As observed in zebrafish (Campos et al. 2012), the *dnmt3* family gene of tongue sole was expanded due to the teleost-specific whole genome duplication (so-called 3R-WGD) followed by lineage-specific duplication of *dnmt3b*, leading to a total of six *dnmt3* paralogues (two *dnmt3a* and four *dnmt3b* compared with mammals). However, the tongue sole genome lacks the ortholog of *dnmt5* in zebrafish, but encodes two *dnmt4* paralogues (named *dnmt4a* and *dnmt4b*, resepctively) instead, indicating that after 3R-WGD, different duplication events of *dnmt3b* have occurred in the tongue sole and zebrafish lineages separately. (**C**) Identity of the dnmt proteins between tongue sole and zebrafish (or human). Protein identities were obtained by BLASTP alignment (Altschul et al. 1997).

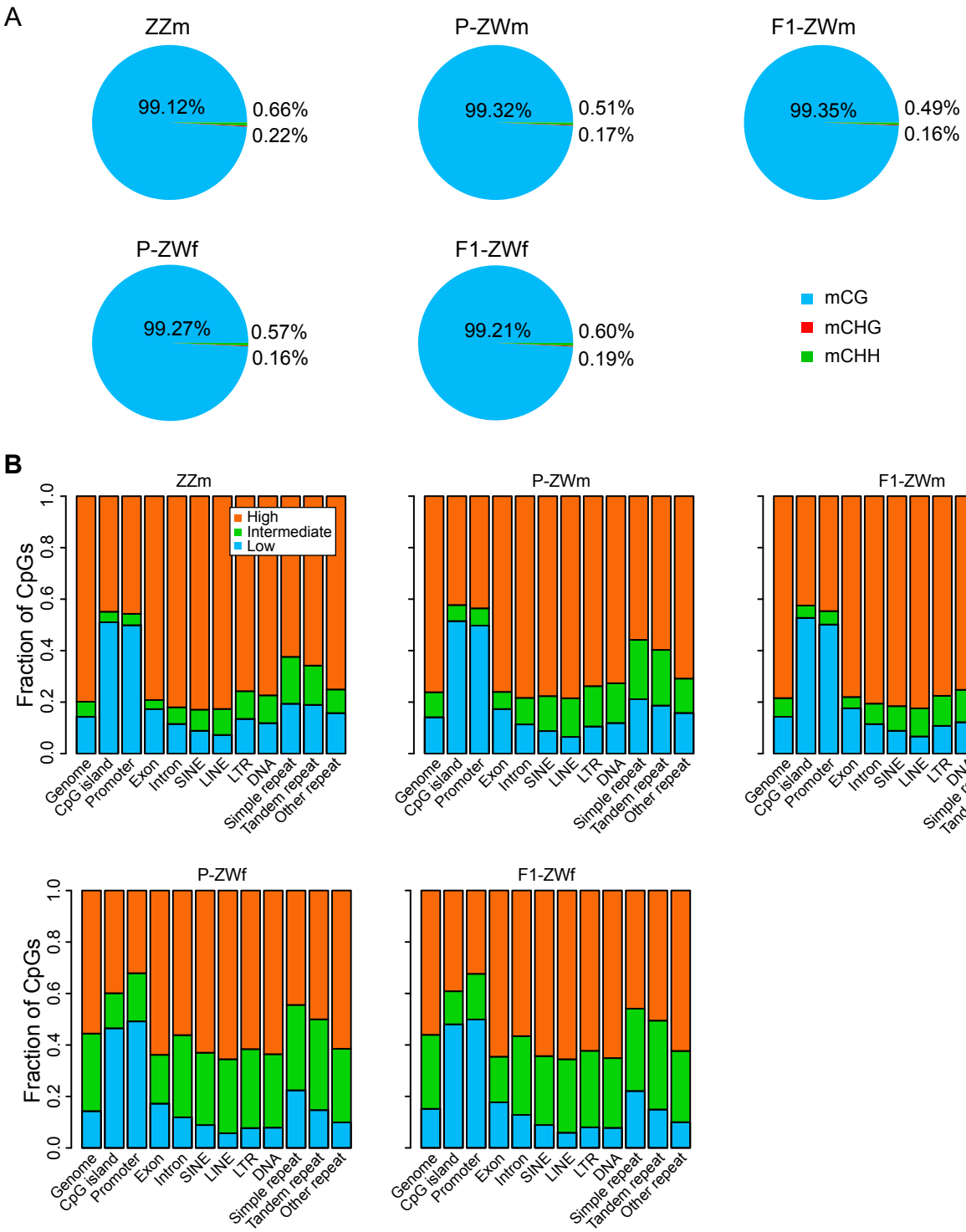

Figure S3. Characteristics of DNA methylation in half-smooth tongue sole. (**A**) Percentage of mCs in CG, CHG and CHH context. (**B**) Fraction of CpG in low (methylation level < 0.25), intermediate (between 0.25 and 0.75) and high (> 0.75) methylation level in different genomic elements.

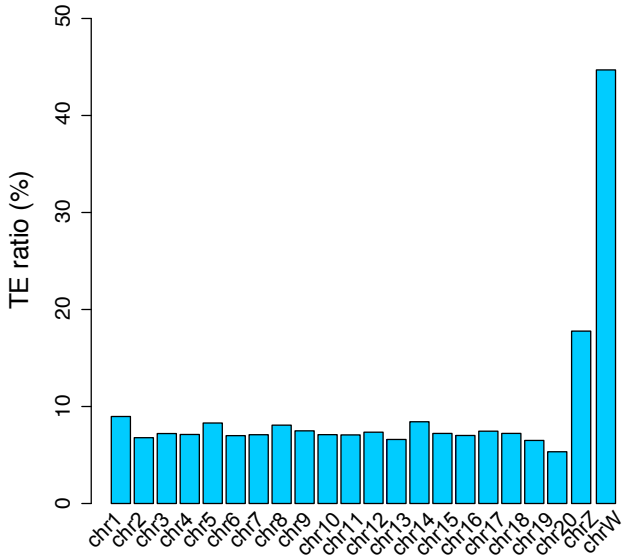

Figure S4. TE ratios in different chromosomes. TE ratio of each chromosome was calculated as dividing the total length of TEs in the chromosome by the length (excluding Ns) of this chromosome.

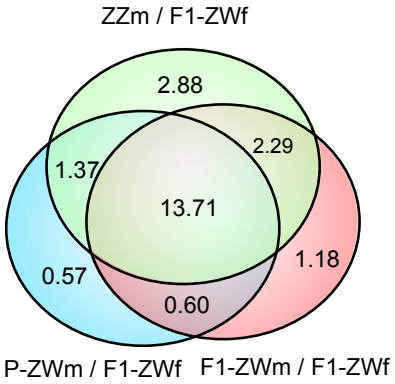

Figure S5. Venn diagrams for DMRs of P-ZWm/F1-ZWf, F1-ZWm/F1-ZWf and ZZm/F1-ZWf. Numbers represent the total length (Mb) of shared DMRs.

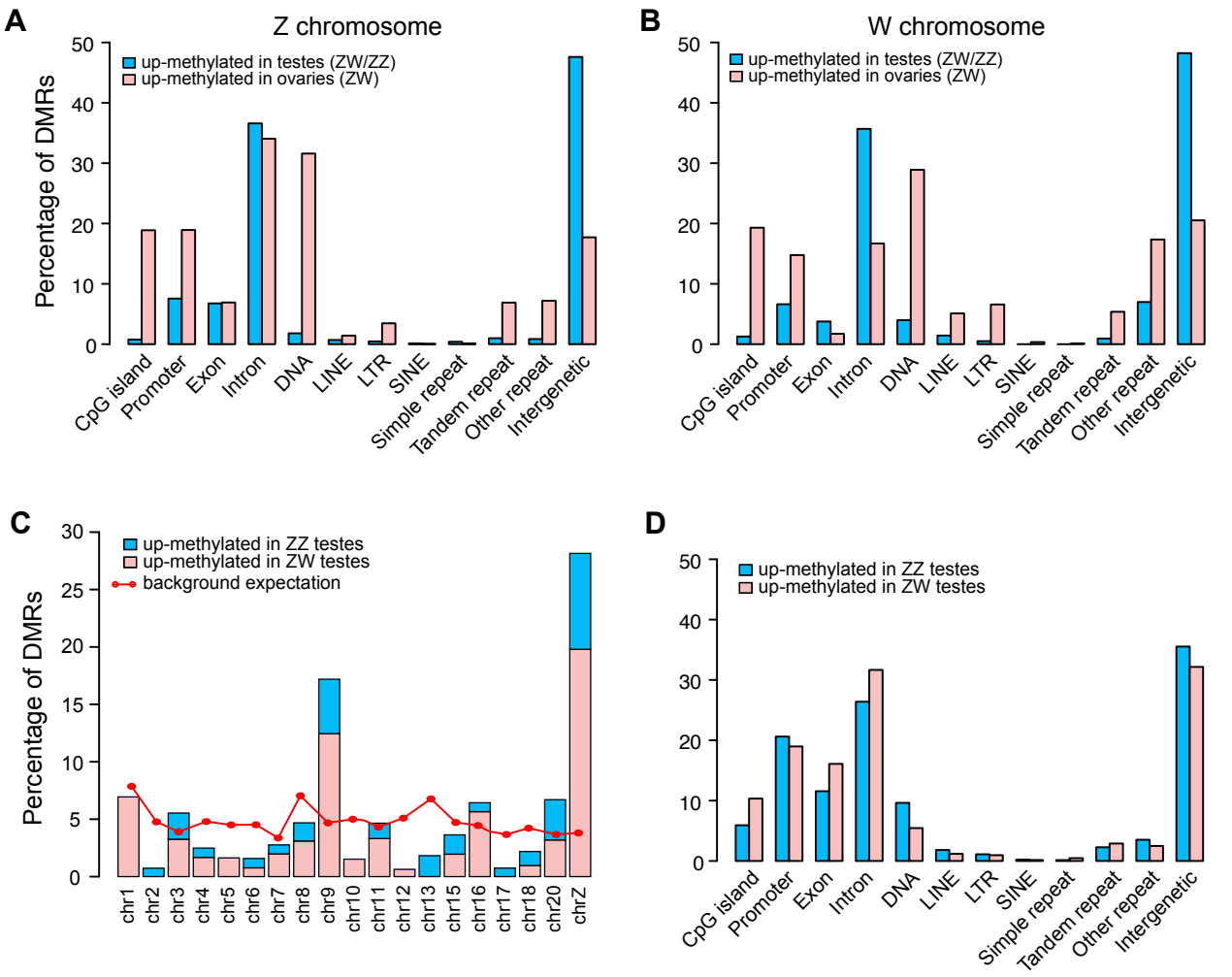

Figure S6. Distribution of DMRs in the tongue sole genome. (**A**) Percentage of Z chromosomal testis/ovary DMRs on different genomic elements. (**B**) Percentage of W chromosomal testis/ovary DMRs on different genomic elements. (**C**) Percentage of ZW-testis/ZZ-testis DMRs on different chromosomes. Background expectation for each chromosome was calculated as the covered length (≥ 6X in P-ZWm, F1-ZWm and ZZm) of each chromosome divided by the total covered length of all chromosomes. (**D**) Percentage of ZW-testis/ZZ-testis DMRs on different genomic elements.

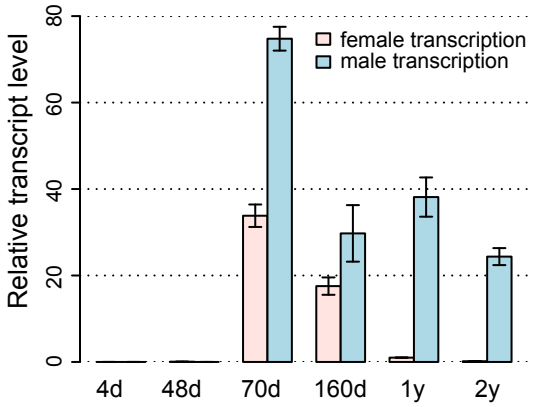

Figure S7. Transcription of *gsdf* in different development stages post hatching.

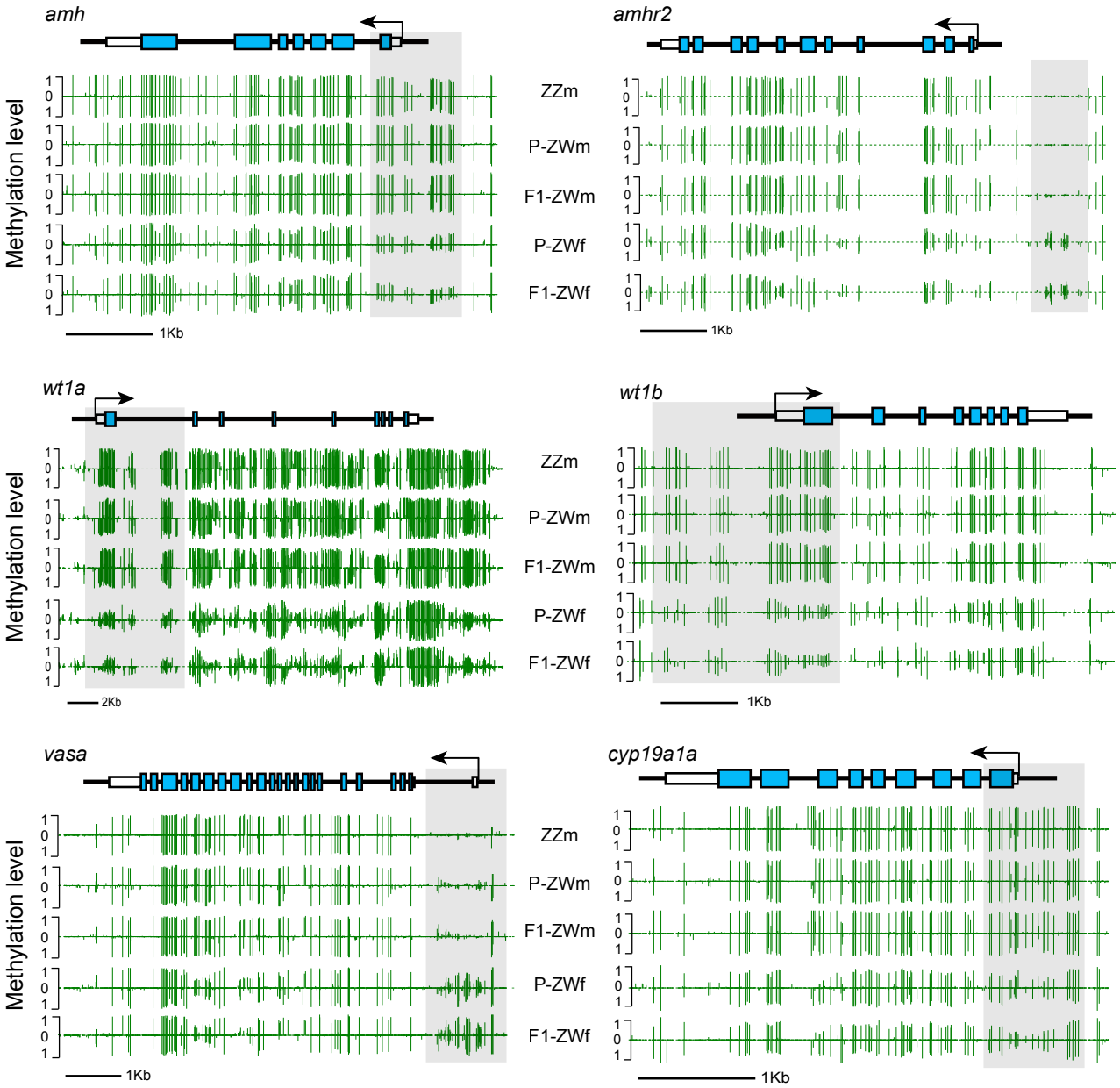
amh
amhr2
wt1a
wt1b
vasa
cyp19a1a
Methylation level
ZZm
P-ZWm
F1-ZWm
P-ZWf
F1-ZWf
1Kb
2Kb

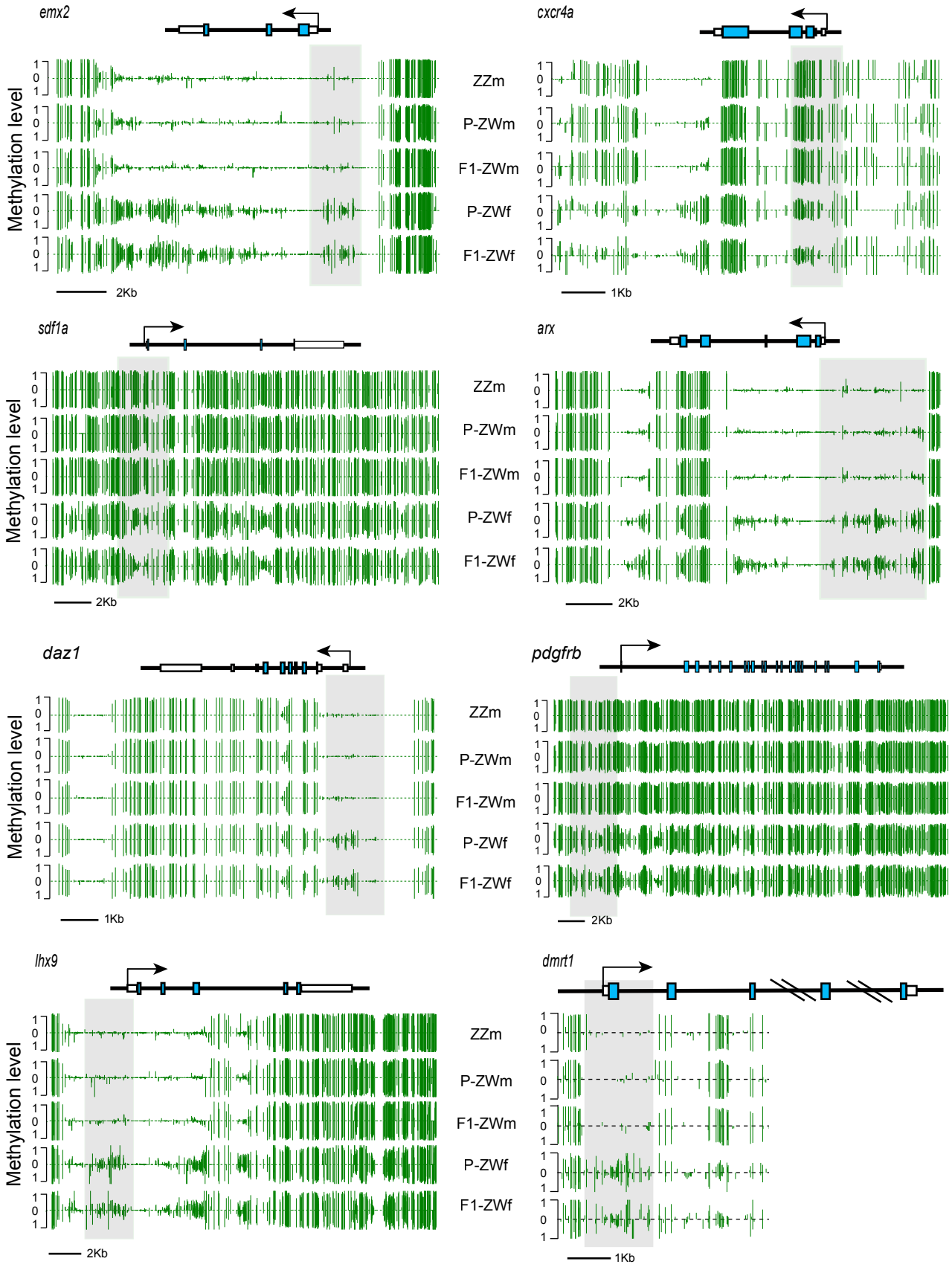

Figure S8. DNA Methylation profiles of *amh, amhr2, wt1a, wt1b, vasa, cyp19a1a, emx2, cxcr4a, sdf1a, arx, daz1, pdgfrb and lhx9* and *dmrt1*. Green vertical lines indicating methylation levels of individual cytosines.

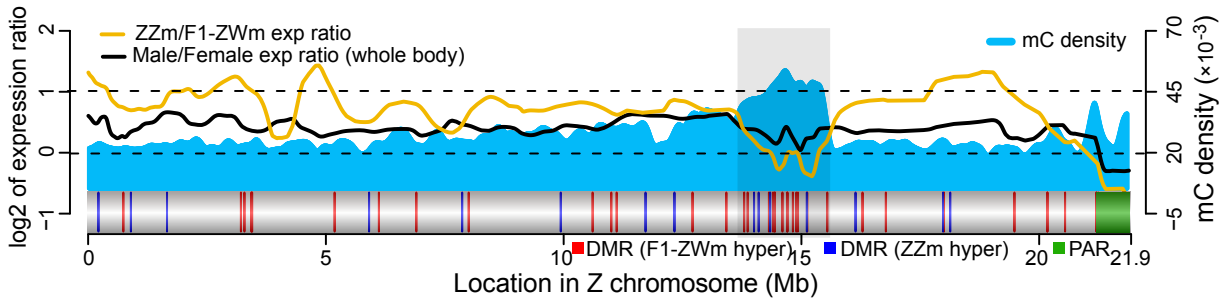

Figure S9. Dosage compensation of the Z chromosome in pseudo-male testes. The same as Figure 4A, but replace P-ZWm by F1-ZWm.

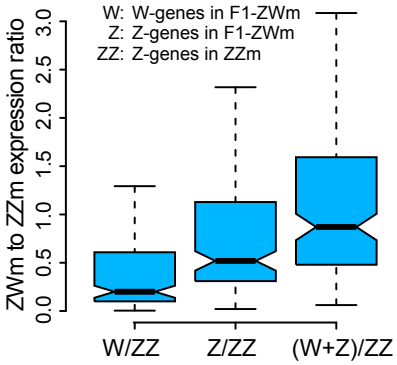

Figure S10. Pseudo-male to normal-male expression ratios calculated from the 272 W-genes and their Z-counterparts. From left to right, 1st box represents expression ratios of F1-ZWm W-genes to ZZm Z-genes, 2nd box represents expression ratios of F1-ZWm Z-genes to ZZm Z-genes, and 3rd box represents expression ratios of the sum of F1-ZWm W- and Z-genes to ZZm Z-genes, indicating that the expression sum of W-Z paralogous genes in pseudo-male testes was close to the dosage of Z-genes in normal males.

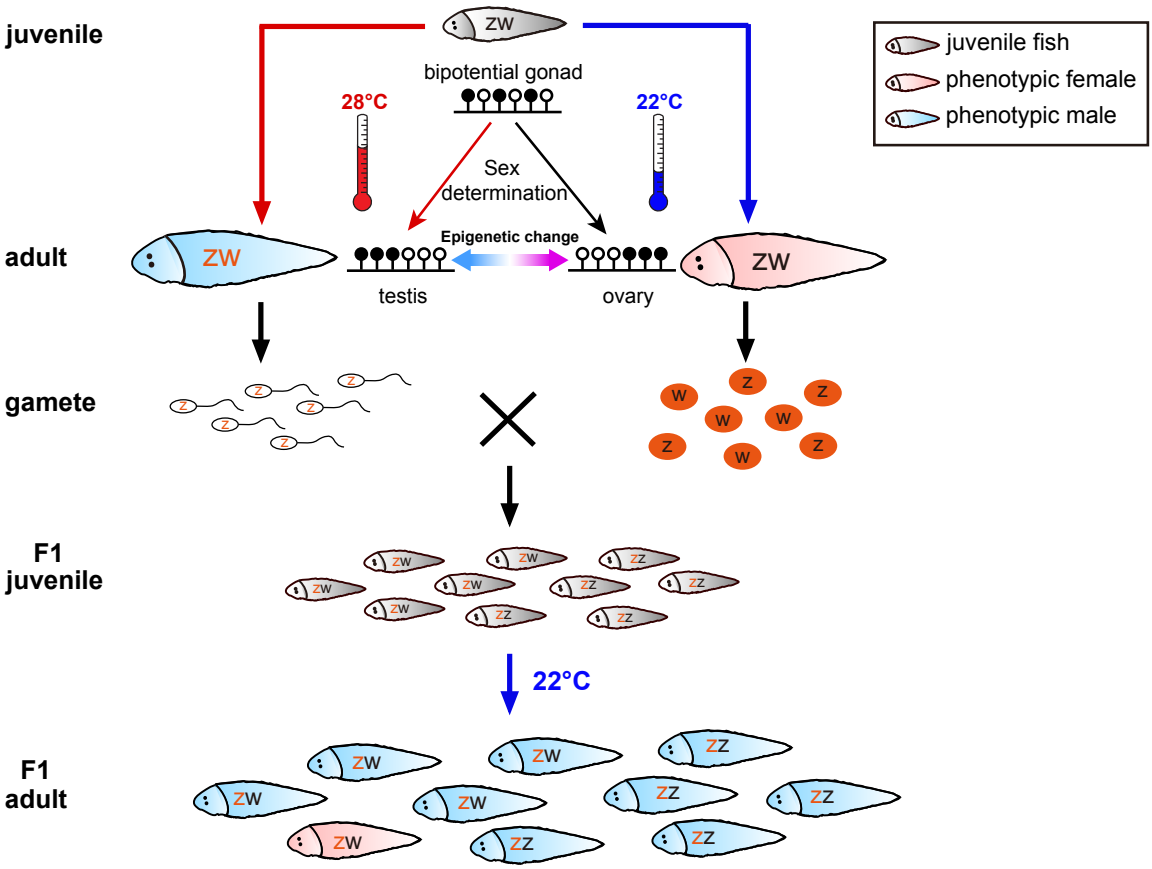

Figure S11. Transgenerational epigenetic inheritance of sexual reversal. We previously demonstrated that the Z chromosomes of F1 ZW fish produced by crossing a pseudo-male with a normal female were exclusively derived from the paternal pseudo-males (Chen et al. 2014), explaining why these F1 ZW fish do not require high temperature induction to express the pseudo-male phenotype. In the present study, we further propose that high temperature treatment of juvenile ZW fish produced by normal crossings can change the epigenetic modification of the Z chromosome, and that some of these alterations are transferred to the next generation, so that most of the F1 genetic females become pseudo-males spontaneously.

Table S1. Gonadal samples for BS-seq and RNA-seq. Sample names were modified from Chen et al. 2014. In this study, we discussed the inheritance of sex reversal in the F1 generation of pseudo-male, thus regarded P-ZWf and P-ZWm as the parental generation and their offsping as F1 generation.

Sample	Genotype	Tissue	BS-seq	RNA-seq	Symbol in this study	Symbol in (Chen et al. 2014)
Parental females	ZW	ovary	√	√	P-ZWf	ZW ovary F1
Parental pseudo-males	ZW	testis	√	√	P-ZWm	ZW ovary F2
F1 females	ZW	ovary	√		F1-ZWf	ZW testis F1
F1 pseudo-males	ZW	testis	√	√	F1-ZWm	ZW testis F2
Normal males	ZZ	testis	√	√	ZZm	ZZ testis P

Table S2. Statistic of BS-seq for each sample.

Sample	Libriary	# Raw reads	# Mapped reads	Mapped ratio (%)	# Unique mapped reads	Unique mapped ratio (%)	Usable depth (X/strand)	Error rate (%)
P-ZWf	CSGjyaHCGDEAAPEM	144,644,160	93420512	64.59	83,756,108	89.65	8	0.46
	CSGjyaHCHDEAAPEM	348,435,048	220670209	63.33	198,174,289	89.81	18	0.49
Sum		493,079,208	314090721	63.70	281,930,397	89.76	26	
F1-ZWf	CSGodeHCDDEAAPEM	162,004,640	105556596	65.16	95,559,961	90.53	9	0.42
	CSGodeHCCDEAAPEM	178,055,666	118688757	66.66	106,940,004	90.1	10	0.43
Sum		340,060,306	224245353	65.94	202,499,965	90.30	19	
P-ZWm	CSGodeHCADEAAPEM	184,809,034	133113099	72.03	120,412,799	90.46	11	0.47
	CSGodeHCBDEAAPEM	195,359,158	131407557	67.26	118,157,554	89.92	11	0.51
Sum		380,168,192	264520656	69.58	238,570,353	90.19	22	
F1-ZWm	CSGjyaHCFDEAAPEM	165,766,754	117360775	70.8	105,567,760	89.95	10	0.50
	CSGjyaHCEDEAAPEM	146,105,060	96539781	66.08	86,955,707	90.07	8	0.55
Sum		311,871,814	213900556	68.59	192,523,467	90.01	18	
ZZm	CSGfttHAGDEAAPEM	173,643,510	130835352	75.35	120,946,405	92.44	11	0.45
	CSGfttHACDEAAPEM	202,483,512	149353932	73.76	137,795,573	92.26	13	0.47
Sum		376,127,022	280189284	74.49	258,741,978	92.35	24	

Table S3. Ratio of cytosines covered by at least 2 reads in each context.

Sample	Covered cytosines(%)			
	C	CG	CHG	CHH
P-ZWf	90.47	91.63	92.43	89.64
F1-ZWf	89.32	90.68	91.50	88.38
P-ZWm	90.15	91.30	92.14	89.32
F1-ZWm	89.51	90.64	91.57	88.65
ZZm	90.23	91.41	92.26	89.37

Table S4. Methylated cytosines detected in each sample.

Sample	Context	# Covered (>=2X)	# Methyl	Ratio (%)
P-ZWf	C	166,975,613	14,701,339	8.8
	CG	17,013,284	14,591,388	85.76
	CHG	40,445,531	24,529	0.06
	CHH	109,516,048	85,422	0.08
F1-ZWf	C	164,852,227	14,442,780	8.76
	CG	16,836,940	14,328,790	85.10
	CHG	40,037,214	27,451	0.07
	CHH	107,977,519	86,539	0.08
P-ZWm	C	166,391,393	14,665,707	8.81
	CG	16,952,463	14,566,134	85.92
	CHG	40,317,332	24,483	0.06
	CHH	109,120,954	75,090	0.07
F1-ZWm	C	165,205,450	14,548,348	8.81
	CG	16,829,003	14,453,261	85.88
	CHG	40,069,206	23,869	0.06
	CHH	108,306,649	71,218	0.07
ZZm	C	161,661,386	14,346,227	8.87
	CG	16,507,031	14,219,773	86.14
	CHG	39,266,490	31,367	0.08
	CHH	105,886,999	95,087	0.09

Table S5. Methylation levels of different chromosomes.

	P-ZWf	F1-ZWf	P-ZWm	F1-ZWm	ZZm	ovary mean	testis mean	testis minus ovary
chr1	0.66	0.66	0.75	0.77	0.78	0.66	0.77	0.11
chr2	0.67	0.67	0.77	0.78	0.79	0.67	0.78	0.11
chr3	0.69	0.69	0.78	0.80	0.81	0.69	0.80	0.11
chr4	0.67	0.67	0.77	0.79	0.80	0.67	0.78	0.11
chr5	0.67	0.67	0.77	0.79	0.80	0.67	0.78	0.11
chr6	0.66	0.66	0.75	0.77	0.78	0.66	0.77	0.11
chr7	0.67	0.67	0.76	0.78	0.79	0.67	0.77	0.11
chr8	0.67	0.68	0.76	0.78	0.79	0.67	0.78	0.10
chr9	0.66	0.66	0.75	0.77	0.77	0.66	0.76	0.10
chr10	0.66	0.66	0.75	0.76	0.78	0.66	0.76	0.10
chr11	0.66	0.66	0.75	0.77	0.78	0.66	0.77	0.11
chr12	0.67	0.67	0.76	0.78	0.79	0.67	0.78	0.11
chr13	0.66	0.66	0.76	0.78	0.78	0.66	0.77	0.11
chr14	0.67	0.68	0.76	0.78	0.79	0.67	0.78	0.11
chr15	0.66	0.66	0.76	0.77	0.78	0.66	0.77	0.11
chr16	0.68	0.68	0.77	0.78	0.79	0.68	0.78	0.10
chr17	0.65	0.65	0.73	0.75	0.76	0.65	0.75	0.10
chr18	0.67	0.67	0.76	0.77	0.78	0.67	0.77	0.10
chr19	0.67	0.67	0.76	0.78	0.79	0.67	0.78	0.10
chr20	0.66	0.66	0.76	0.77	0.78	0.66	0.77	0.11
chrZ	0.67	0.67	0.74	0.75	0.77	0.67	0.75	0.08
chrW	0.73	0.73	0.75	0.77	0.00	0.73	0.76	0.03
genome	0.67	0.67	0.76	0.78	0.78	0.67	0.77	0.10

Table S6. GO enrichment for DMGs up-methylated in ovaries.

GO ID	GO Term	Gene Num	P value	GO Level
reproductive developmental process				
GO:0045137	development of primary sexual characteristics	17	4.91×10^{-3}	4
GO:0046660	female sex differentiation	13	8.26×10^{-3}	4
GO:0046545	development of primary female sexual characteristics	12	1.51×10^{-2}	5
GO:0048608	reproductive structure development	17	2.92×10^{-2}	4
GO:0008585	female gonad development	10	3.21×10^{-2}	6
sexual reproduction				
GO:0007276	gamete generation	26	2.40×10^{-3}	4
GO:0007292	female gamete generation	10	1.40×10^{-2}	5
GO:0048477	oogenesis	8	1.80×10^{-2}	6
GO:0034587	piRNA metabolic process	3	1.94×10^{-2}	7
GO:0007283	spermatogenesis	18	1.94×10^{-2}	6
GO:0007140	male meiosis	4	4.36×10^{-2}	6
meiosis				
GO:0000279	M phase	28	3.11×10^{-3}	5
GO:0007126	meiosis	12	3.75×10^{-3}	5
GO:0007129	synapsis	4	1.07×10^{-2}	5
GO:0007127	meiosis I	7	1.68×10^{-2}	5
pattern specification process				
GO:0003002	regionalization	40	1.36×10^{-10}	4
GO:0009952	anterior/posterior pattern specification	30	6.48×10^{-10}	5
other developmental process				
GO:0048706	embryonic skeletal system development	22	8.36×10^{-11}	6
GO:0009792	embryo development ending in birth or egg hatching	46	1.19×10^{-6}	4
GO:0043009	chordate embryonic development	45	2.60×10^{-6}	5
GO:0048732	gland development	28	5.97×10^{-6}	5
GO:0030326	embryonic limb morphogenesis	17	7.74×10^{-4}	6
GO:0061138	morphogenesis of a branching epithelium	17	2.51×10^{-3}	4
GO:0042471	ear morphogenesis	15	5.46×10^{-3}	6
GO:0021615	glossopharyngeal nerve morphogenesis	3	6.39×10^{-3}	5
GO:0035136	forelimb morphogenesis	9	1.57×10^{-2}	6
GO:0051216	cartilage development	17	1.80×10^{-2}	5
GO:0021545	cranial nerve development	8	2.68×10^{-2}	5
GO:0055123	digestive system development	14	2.92×10^{-2}	5
GO:0021983	pituitary gland development	8	3.59×10^{-2}	5
GO:0043010	camera-type eye development	23	4.17×10^{-2}	7

Table S7. GO enrichment for DMGs up-methylated in testes (ZW/ZZ).

GO ID	GO Term	Gene Num	P value	GO Level
response to chemical stimulus				
GO:0070887	cellular response to chemical stimulus	224	5.19×10^{-5}	4
GO:0070482	response to oxygen levels	57	4.20×10^{-4}	4
GO:0010033	response to organic substance	261	2.42×10^{-3}	4
GO:0071383	cellular response to steroid hormone stimulus	29	3.86×10^{-3}	6
GO:0006935	chemotaxis	117	3.88×10^{-3}	4
GO:0006979	response to oxidative stress	49	5.06×10^{-3}	4
GO:0071375	cellular response to peptide hormone stimulus	59	1.50×10^{-2}	6
GO:0000302	response to reactive oxygen species	29	1.52×10^{-2}	5
developmental process				
GO:0001944	vasculature development	139	1.83×10^{-8}	5
GO:0072358	cardiovascular system development	197	4.51×10^{-8}	5
GO:0001525	angiogenesis	95	1.67×10^{-6}	4
GO:0060429	epithelium development	138	1.43×10^{-5}	5
GO:0007431	salivary gland development	20	1.07×10^{-4}	6
GO:0007507	heart development	107	3.07×10^{-4}	5
GO:0035272	exocrine system development	24	1.87×10^{-3}	5
GO:0048729	tissue morphogenesis	116	2.88×10^{-3}	4
GO:0030865	cortical cytoskeleton organization	11	3.98×10^{-3}	7
GO:0031099	regeneration	41	4.57×10^{-3}	4
GO:0048812	neuron projection morphogenesis	129	7.68×10^{-3}	7
GO:0060027	convergent extension involved in gastrulation	17	8.83×10^{-3}	5
GO:0035088	establishment or maintenance of apical/basal cell polarity	13	1.13×10^{-2}	5
GO:0060485	mesenchyme development	45	1.52×10^{-2}	5
GO:0061061	muscle structure development	100	2.14×10^{-2}	4
GO:0060539	diaphragm development	6	2.14×10^{-2}	6
GO:0048659	smooth muscle cell proliferation	19	2.42×10^{-2}	4
GO:0072110	glomerular mesangial cell proliferation	6	3.38×10^{-2}	4
GO:0001890	placenta development	27	4.21×10^{-2}	5
cellular component organization				
GO:0000902	cell morphogenesis	190	9.02×10^{-4}	5
GO:0030036	actin cytoskeleton organization	88	1.16×10^{-3}	4
GO:0030010	establishment of cell polarity	21	6.61×10^{-3}	4
GO:0008360	regulation of cell shape	23	9.04×10^{-3}	4
GO:0034329	cell junction assembly	42	1.34×10^{-2}	4
GO:0007015	actin filament organization	44	1.58×10^{-2}	5
signal transduction				
GO:0009966	regulation of signal transduction	296	1.25×10^{-6}	4
GO:0007167	enzyme linked receptor protein signaling pathway	179	7.92×10^{-6}	5
GO:0043405	regulation of MAP kinase activity	59	2.99×10^{-4}	5
GO:0071902	positive regulation of protein serine/threonine kinase activity	54	2.99×10^{-4}	9
GO:0007166	cell surface receptor signaling pathway	371	3.20×10^{-4}	4
GO:0043401	steroid hormone mediated signaling pathway	21	2.92×10^{-3}	5
GO:0043408	regulation of MAPK cascade	63	4.81×10^{-3}	6
GO:0007243	intracellular protein kinase cascade	128	5.39×10^{-3}	5
GO:0007266	Rho protein signal transduction	39	5.99×10^{-3}	7

GO:0046578	regulation of Ras protein signal transduction	68	7.00×10^{-3}	6
GO:0070374	positive regulation of ERK1 and ERK2 cascade	21	9.46×10^{-3}	7
GO:0071526	semaphorin-plexin signaling pathway	8	1.15×10^{-2}	5
GO:0007264	small GTPase mediated signal transduction	107	1.52×10^{-2}	5
GO:0048008	platelet-derived growth factor receptor signaling pathway	13	1.60×10^{-2}	7
GO:0070431	nucleotide-binding oligomerization domain containing 2 signaling pathway	4	2.51×10^{-2}	7
GO:0050852	T cell receptor signaling pathway	19	2.87×10^{-2}	7
GO:0070427	nucleotide-binding oligomerization domain containing 1 signaling pathway	3	4.08×10^{-2}	7
biological regulation				
GO:2000026	regulation of multicellular organismal development	207	5.73×10^{-7}	4
GO:0009966	regulation of signal transduction	296	1.25×10^{-6}	4
GO:0045595	regulation of cell differentiation	181	1.19×10^{-5}	4
GO:0045860	positive regulation of protein kinase activity	85	2.13×10^{-4}	8
GO:0042325	regulation of phosphorylation	152	3.03×10^{-4}	7
GO:0010952	positive regulation of peptidase activity	32	4.20×10^{-4}	7
GO:0033674	positive regulation of kinase activity	87	4.52×10^{-4}	7
GO:0060284	regulation of cell development	106	1.84×10^{-3}	5
GO:0010906	regulation of glucose metabolic process	22	2.24×10^{-3}	6
GO:0019220	regulation of phosphate metabolic process	155	2.84×10^{-3}	6
GO:0001558	regulation of cell growth	57	2.88×10^{-3}	4
GO:0043065	positive regulation of apoptotic process	109	5.32×10^{-3}	6
GO:0044093	positive regulation of molecular function	190	6.19×10^{-3}	4
GO:0008360	regulation of cell shape	23	9.04×10^{-3}	4
GO:0050795	regulation of behavior	30	2.20×10^{-2}	4
GO:0050920	regulation of chemotaxis	23	3.12×10^{-2}	4
GO:0010646	regulation of cell communication	213	3.53×10^{-2}	4

Table S8 (See excel document). Expression and methylation of genes related to sex differentiation. For gene expression, genes were categorized into testis-biased (T), ovary-biased (O) and non-biased (N) expression based on RPKM fold changes (FC) between P-ZWf and the mean value of P-ZWm, F1-ZWm and ZZm. Fold change (FC) > 1.5 was chosen as the significant threshold. For DNA methylation, genes were categorized into testis-up-methylated (T), ovary-up-methylated (O) and no significant difference (N) based on whether the promoter region of a given gene harbored identified DMR. DNA methylation profiles of the 16 genes with promoter DMRs are presented in Figure 3C (*gsdf*), Figure 5D (*figla*) and Figure S8 (the rest 14 genes). This table is modified from table S43 in Chen et al. 2014.

Table S9 (See excel document). Dosage compensated Z-genes in pseudo-male testes relative to normal male testes. Genes were defined as dosage compensation if RPKM ratio of ZZm/P-ZWm or ZZm/F1-ZWm is between 1/1.5 and 1.5.

Table S10. Primers for BS-PCR and RT-PCR experiments.

Experiment	Gene	Tm (°C)	Primer Sequence 5'-3'
BS-PCR	*dmrt1*	48	F: GGTTAAATATTGTTATAGTAGTAGTAG R: ACRATTACCTACACCACCA
RT-PCR	*gsdf*	60	F: TTCTTCGGTTGTGCTTGCG R: CGGCTCAGTCTGGAGGTTCA
	figla AFE1-2nd	58	F: ACATAGAGAAGTTCAAACGAGCC R: CGGTAGCAGCTTTTAGTGTGTCT
	figla AFE2-3rd	60	F: AACCTCTCGTCTTCACTCCTCTCTC R: TCCCTAGGCCTTCAGTCTGG

Supplemental Experimental Procedures

Gene Ontology Annotated and Enrichment Analysis

Gene ontology (GO) categories of the tongue sole genes were annotated based on homologous relationships between tongue sole genes and that of zebra fish (*Danio rerio*), Medaka (*Oryzias latipes*) and human (*Homo sapiens*) downloaded from Ensembl (Flicek et al. 2012). Briefly, we first mapped all the tongue sole proteins to the protein sets of these three species separately using BLASTP (Altschul et al. 1990), then GO annotations were assigned for the tongue sole genes according to GO annotations of their best hits in these three species. We required the aligning rate of each tongue sole gene to its best hit must exceed 30%, and the GO annotations from these three species were finally merged to a non-redundant result.

Fisher's Exact Test and Chi-squared Test (Beißbarth and Speed 2004) was employed to estimate whether a list of genes (foreground genes, e.g. DMGs) was enriched in a specific GO category when compared with background genes. P-values were adjusted for multiple testing by consideration of the Benjamini-Hochberg False Discovery Rate (Benjamini et al. 2001), and the adjusted P-value < 0.05 was chosen as the significant threshold.

Methylation Analysis of *Dmrt1* by Bisulfite-PCR

To track the DNA methylation status of *dmrt1* during gonadal development, we performed bisulfite-PCR for genomic DNA extracted from genetic female and male gonads at different developmental stages, including 4 days post-hatching (dph), 25 dph, 48 dph, 70 dph, 160 dph, 8 m, 10 m, 1 y and 2 y. DNA were extracted using Genomic DNA Extraction Kit (TAKARA). Bisulfite-PCR primers were designed on the first exon of *dmrt1* using Primer Premier 5 (Table S10). For PCR amplification, a 40 μl reaction system was carried out with 1X PCR buffer, 5 mM $MgCl_2$, 1 mM dNTP mix, 1 unit of Taq polymerase, 50 pmol of the forward primer and reverse primer respectively, and 50 ng of bisulfite-treated DNA. The PCR cycling conditions were 94 °C for 1 min, followed by 40 cycles of [94 °C for 30 s, 50 °C for 30 s and 72 °C for 30 s], followed by 72 °C for 5 min and stored at 4 °C. PCR products were electrophoresed on 1% agarose gels, followed by bands excised and gel extracted using the Zymoclean Gel DNA Recovery Kit. Purified PCR products were cloned using the pMD18-T Simple Vector cloning kit following the manufacturer's protocol. For each sample, we randomly selected no less than 15 clones for sequencing. All sequencings were performed on an ABI 3730xl DNA analyzer using SP6 or T7 primers.

Expression of *Dmrt1* and *Gsdf* at Different Developmental Stages

RT-PCR analysis results of *dmrt1* at different developmental stages were obtained from Chen S et al (Chen et al. 2014) by adding the data of two additional time points (8 m and 10 m) using the 1 y sample as control (Chen et al. 2014). For *gsdf*, total RNA of female and male gonads at different developmental stages (4 dph, 48 dph, 70 dph, 160 dph, 1 y, 2 y) were extracted from another batch of fish and reverse transcribed as described previously (Chen et al. 2001). Primers for RT-PCR analysis of *gsdf* were designed using the Primer3 program (Rozen and Skaletsky 2000) (Table S10). The final PCR reactions contained 0.4 mM of each primer, 10 μl SYBR Green (Invitrogen) and 80 ng template (cDNA reverse transcribed from a standardized amount of total RNA). RT-PCR was performed on ABI PRISM 7500 Real-Time PCR System using Hotstart Taq polymerase (Qiagen) in a final volume of 20 μl and β-actin gene was used as internal reference. All reactions were subjected to: 95°C for 35 s followed by 40 cycles at 95°C for 5 s, 60°C 34 s. Melting curve analysis was applied to all reactions to ensure homogeneity of the reaction product. RT-PCR results were analyzed using 7500 System SDS Software.

Alternative Splicing and Expression of *Figla*

Additional gonadal RNA extracted from adult fish, including two females, two normal males and two pseudo-males were used for confirming the existence and abundance of the two splicing forms of *figla* in tongue sole. We designed two pairs of primers, spanning AFE1-2nd exon and AFE2-3rd exon respectively (Figure 5D and Table S10). PCRs were performed on all the six samples, followed by agarose gel electrophoresis. As expected, we could not observe any bands in normal male samples, while in female and pseudo-male samples, we observed bands corresponding to these two pair of primes with expected fragment sizes. Then we also performed RT-PCR on all the six samples to test the relative abundances of the two splicing forms in different samples. RT-PCR were performed with the same protocol as described above.

Supplemental References

Altschul SF, Gish W, Miller W, Myers EW, Lipman DJ. 1990. Basic local alignment search tool. *J Mol Biol* **215**(3): 403-410.

Altschul SF, Madden TL, Schaffer AA, Zhang J, Zhang Z, Miller W, Lipman DJ. 1997. Gapped BLAST and PSI-BLAST: a new generation of protein database search programs. *Nucleic acids research* **25**(17): 3389-3402.

Beißbarth T, Speed TP. 2004. GOstat: find statistically overrepresented Gene Ontologies within a group of genes. *Bioinformatics* **20**(9): 1464-1465.

Benjamini Y, Drai D, Elmer G, Kafkafi N, Golani I. 2001. Controlling the false discovery rate in behavior genetics research. *Behav Brain Res* **125**(1-2): 279-284.

Campos C, Valente LMP, Fernandes JMO. 2012. Molecular evolution of zebrafish dnmt3 genes and thermal plasticity of their expression during embryonic development. *Gene* **500**(1): 93-100.

Chen S, Hong Y, Scherer SJ, Schartl M. 2001. Lack of ultraviolet-light inducibility of the medakafish (Oryzias latipes) tumor suppressor gene p53. *Gene* **264**(2): 197-203.

Chen S, Zhang G, Shao C, Huang Q, Liu G, Zhang P, Song W, An N, Chalopin D, Volff J et al. 2014. Whole-genome sequence of a flatfish provides insights into ZW sex chromosome evolution and adaptation to a benthic lifestyle. *Nat Genet* doi: 10.1038/ng.2890.

Flicek P, Amode MR, Barrell D, Beal K, Brent S, Carvalho-Silva D, Clapham P, Coates G, Fairley S, Fitzgerald S. 2012. Ensembl 2012. *Nucleic acids research* **40**(D1): D84-D90.

Rozen S, Skaletsky H. 2000. Primer3 on the WWW for general users and for biologist programmers. *Methods Mol Biol* **132**: 365-386.

Wu H, Caffo B, Jaffee HA, Feinberg AP, Irizarry RA. 2010. Redefining CpG islands using hidden Markov models. *Biostatistics* **11**(3): 499-514.